Journal of Industrial and Engineering Chemistry 20 (2014) 1623–1632

Contents lists available at ScienceDirect

Journal of Industrial and Engineering Chemistry

journal homepage: www.elsevier.com/locate/jiec

Nano-SiO_2/fluorinated waterborne polyurethane nanocomposite adhesive for laminated films

Heqing Fu *, Caibin Yan, Wei Zhou, Hong Huang

School of Chemistry and Chemical Engineering, South China University of Technology, Guangzhou 510640, China

ARTICLE INFO

Article history:
Received 4 May 2013
Received in revised form 26 June 2013
Accepted 5 August 2013
Available online 1 September 2013

Keywords:
Empirical model
Waterborne polyurethane
Nanocomposite adhesive
Laminated films
Adhesion strength

ABSTRACT

High performance nanocomposite adhesives used for the laminated films were synthesized. The effects of nano-SiO_2 and HFBMA contents on the properties of SiO_2/FWPU nanocomposite adhesive were investigated by the static contact angle measurement, X-ray photoelectron spectroscopy, atomic force microscopy, thermogravimetric analysis and tensile test machine. It proved that the wetting behavior, water resistance and thermal stability of nanocomposite adhesive had effect on the adhesion of the nanocomposite adhesive for low surface energy materials. And an empirical equation, $T = e^{32.04} \times \gamma_L^{-8.08} \times \gamma_S^{0.45}$, revealing the relationship among adhesion strength (T), surface tension of adhesive (γ_L)and the surface energy of adhered substrate (γ_S)was obtained.

1. Introduction

Nonpolar polyolefin films, such as polyethylene (PE), biaxially oriented polypropylene (BOPP) and cast polypropylene (CPP), are widely used in the soft package of food, medicine, household and so on. In order to fit the need of soft packages, these films should be adhered together by adhesive [1]. However, they are difficult to bond due to their nonpolarity and low surface free energy. Therefore, the surface polarity of polyolefin films need to be improved. Some methods, such as plasma, corona discharge, electronic radiation, acid etching and so on, appear to improve the surface polarity of polyolefin films [2–7]. Particularly the corona discharge method appears to be the most convenient approaches. When polyolefin films were treated by the corona discharge, the carbonyl groups and carboxyl groups were generated on the surface of polyolefin films, their surface polarity can be improved and their surface energy can be enhanced to 38–40 mN/m [8].

The solvent-borne polyurethane (PU) adhesive is widely used due to the excellent adhesive strength, water resistance and thermal stability. However, its use in the laminated soft package industry is restricted for emission of volatile organic compound (VOC) causing problems like toxicity, flammability and pollution. Waterborne polyurethane (WPU) adhesive overcomes these problems, and thus takes the place of the solvent-borne PU adhesive in the laminated soft package industry [9,10]. However, the poor wettability, heat resistance, and inferior water resistance of the WPU, it needs to be modified to ensure its application in the soft package.

Nano-SiO_2 is often used in polymer composites [11–14]. For this purpose, its compatibility with the polymer matrix should be modified. Different surface modifiers such as coupling agents, surfactants, aliphatic acids, and so on, have been used in surface modification of nano-SiO_2 [15–18]. Among them, the silane coupling agents are one of the best due to the alkoxy groups of silane coupling agent are able to react with the surface silanol groups of nano-SiO_2, and the organic functional groups which contained amino, epoxy and acrylic functionality, can react with the –NCO groups in the PU chains. The formation of stable chemical linkages between the nano-SiO_2 and the polymer improve the heat resistance, radiation resistance and mechanical properties of WPU.

On the other hand, fluorine acrylic has relatively low surface energy due to the low polarizability and the strong electronegativity of fluorine atom [19–21]. Fluorine acrylic is widely used in the fluorinate waterborne polyurethane (FWPU) hybrid emulsion via emulsion polymerization. Compared to the conventionally prepared WPU dispersion, the FWPU hybrid emulsion exhibits good wettability to the low surface energy substrates. In addition, the surface properties of the FWPU films can also be significantly improved with the incorporation of fluorinate acrylic.

Theoretically, multiple approaches have been given to explain the complex adhesion mechanism, including the absorption

* Corresponding author. Tel.: +86 20 87114919; fax: +86 20 87112047.
E-mail address: fuhq@scut.edu.cn (H. Fu).

1226-086X/$ – see front matter © 2013 The Korean Society of Industrial and Engineering Chemistry. Published by Elsevier B.V. All rights reserved.
http://dx.doi.org/10.1016/j.jiec.2013.08.009

theory, the electrostatic theory, the diffusion theory, the mechanical bonding theory, the chemical bonding theory, the coordination bond theory, and so on [22–25]. Unfortunately, none of them could completely explain all of the existed adhesion phenomenons due to their limited applying conditions and the complexity of theoretical models. And the adhesion mechanism in the adhesion process is still no clear currently.

Hence, in this work a series of nano-SiO_2/fluorinated waterborne polyurethane (SiO_2/FWPU) nanocomposite emulsions with core–shell particle structure modified by nano-SiO_2 (treated by 3-aminopropyltriethoxysilane) and 2,2,3,4,4,4-hexafluorobutyl methacrylate (HFBMA) were synthesized. A high performance nanocomposite adhesive was made through the SiO_2/FWPU nanocomposite emulsion. The influences of wettability, water resistance and thermal stability of nanocomposite adhesive on the adhesion strength were examined.

Although there are some reports about the WPU modified by either fluorinated acrylic or modified nano-SiO_2, there is no report about preparing and characterizing nano-SiO_2/fluorinated waterborne polyurethane (SiO_2/FWPU) nanocomposite adhesive modified by nano-SiO_2 and fluorinated acrylic at the same time. Moreover, the SiO_2/WPU hybrid dispersions were used as seed emulsion and internal reactive macromolecule emulsifier instead of adding traditional emulsifier. As a result, the bad effect of traditional emulsifier defect on the properties of nanocomposites has got rid of.

On the other hand, it proves that the adhesion process of the adhesive to the adhered substrates is a complex physicochemical process, and the adhesion strength depends strongly on the interface interaction between the adhesive and the adhered substrates [26–28]. In relation to these observations, we developed an empirical model that incorporated the adhesion strength, the surface tension of nanocomposite adhesive and the surface energy of adhered substrate together. And a new empirical equation was obtained via multiple linear regressions to present a possible correlation among these three parameters. There is no report about this research.

2. Experimental

2.1. Materials

Nano-SiO_2 (supplied by Degussa, Germany) was modified by 3-aminopropyltriethoxysilane (APTES) through surface chemical modification in situ [15]; isophorone diisocyanate (IPDI), 1,4-butylene adipate glycol (PBA, Mn = 2000), acetone (supplied by Donghao Resine Co. Ltd., China), dimethylol propionic acid (DMPA) (supplied by Perstop, Sweden), ethanol, *n*-methyl pyrrolidone (NMP) and triethylamine (TEA) (supplied by Shanghai Fine Chemical Agent Factory, China), dibutyltin dilaurate (DBTDL) (supplied by Shanghai Lingfeng Chemical Agent Co. Ltd, China), 2-hydroxyethyl acrylate (HEA) and 2,2,3,4,4,4-hexafluorobutyl methacrylate (HFBMA) (supplied by Harbin Xeogia Fluorine-Silicon Chemical Co., Ltd.), sodium bicarbonate ($NaHCO_3$) and ammonium persulfate (APS) (supplied by Shanghai Chemical Reagent Co., Ltd.).

2.2. Preparation of the SiO_2/WPU hybrid dispersion

The SiO_2/WPU hybrid dispersions were prepared by prepolymer process, as shown in Fig. 1. A dry 1000 mL four-necked glass reaction kettle equipped with a mechanical stirrer, thermometer, condenser and a nitrogen inlet was placed in a water bath. The stoichiometric PBA was dried at 110 °C for 1.5 h in a vacuum oven, IPDI and the catalyst DBTDL were added into the reactor under N_2 atmosphere, and the reaction was carried out at 80 °C for 2 h. After that, DMPA dissolved in NMP was added into the kettle where the reaction temperature was 75 °C. Then, modified nano-SiO_2 (in weight fraction of 0, 0.5, 1, 1.5, 2 wt%) was added into the reactor to react for 2 h. The reaction proceeded until the residual NCO reached the expected content (determined by the standard dibutylamine back-titration method [29]). After the prepolymer was cooled to 50 °C, HEA was added to end-cap the prepolymer and the reaction continued for 2 h. The carboxylic acid in the prepolymer was neutralized by TEA solution for 30 min at 40 °C to obtain ionomer (before the neutralization, a little amount of acetone was added to adjust the viscosity of the prepolymer). The ionomer was dispersed into the stoichiometric amount of deionized water with vigorous stirring. The SiO_2/WPU hybrid dispersion with a solid content of 30 wt% was finally obtained after removing the acetone by vacuum distillation.

2.3. Synthesis of the SiO_2/FWPU nanocomposite emulsions

The SiO_2/FWPU nanocomposite emulsions were synthesized via seed emulsion polymerization process by using SiO_2/WPU hybrid dispersion as seed emulsion and macromonomer, fluorinated acrylic HFBMA, as presented in Fig. 2. The SiO_2/WPU hybrid dispersion and deionized water were added into a reaction kettle under high speed stirring to obtain a stable emulsion. The pH value of the emulsion was adjusted to 8 by adding $NaHCO_3$. Then, HFBMA was added into the mixture solution with vigorous stirring for 30 min, and the temperature is up to 80 °C. Then the $(NH_4)_2S_2O_4$ dissolved in water with mass concentration of 0.5 wt% was dropped into the reactor in 3 h. After heating for another 2 h, the emulsions were cooled down to 40 °C and the SiO_2/FWPU nanocomposite emulsions were finally obtained. The compositions of SiO_2/FWPU nanocomposite emulsions were shown in Table 1. The nanocomposite adhesives were ultimately obtained by adding predetermined amount of assistants into the nanocomposite emulsions.

2.4. Film preparation

The nanocomposite films were prepared by casting the nanocomposite emulsion on a PTFE mould dried at room temperature for 7 days. Then the films were placed in a vacuum oven at 60 °C for 24 h before characterization.

2.5. Characterization

Differential scanning calorimetry (DSC) analysis was measured by a TA Instruments Q20 DSC analyzer over the range from −60 to 150 °C at a heating rate of 10 °C/min under N_2 atmosphere.

The surface tension of nanocomposite emulsions was measured with the pendant drop apparatus affiliated to the contact angle goniometer (JC2000C1 Powereach®, Shangai Zhongchen) using the pendant-drop method at 25 °C. Samples for surface tension measurement were the polymer solutions in deionized water with different polyurethane content. The reported results were the average of three measurements. While the contact angles were measured by the JC2000C1 using the sessile-drop method at 25 °C. The reported values were the average of three replicates.

The water swelling of nanocomposite films was measured by immersing the nanocomposite films in deionized water, and the degree of swelling was calculated by the following formula:

$$Swelling\% = \frac{m_1 - m_0}{m_0} \times 100\% \quad (1)$$

where m_0 and m_1 are the mass of dry film and the wet film which immersed in water for 24 h, respectively.

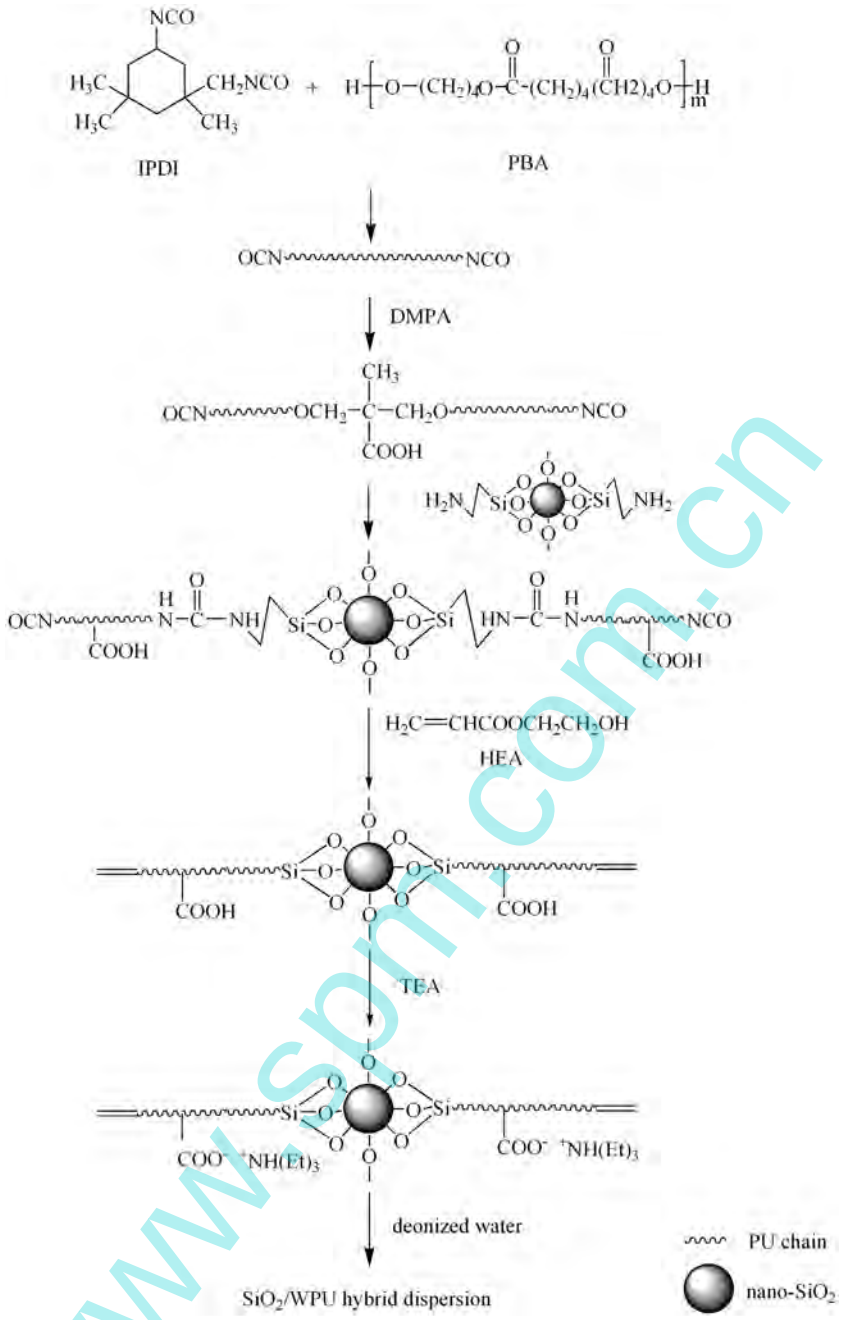

Fig. 1. Flowchart of the preparation of SiO_2/WPU hybrid dispersion.

The surface chemical compositions of nanocomposite on the air-film interface were determined by X-ray photoelectron spectrometer (VG Scientific, ESCA LAB MK II) equipped with Alka achromatic X-ray source.

The atomic force microscopy (AFM) measurement was performed on the instrument (CSPM 2003) with 10 μm × 10 μm scan area and images were acquired under ambient conditions in tapping mode using a nanoprobe cantilever.

The thermogravimetric analysis (TGA) was investigated by STGA 449C (Netzsch, Germany) with a heating rate of 10 °C/min from 60 to 600 °C under a N_2 atmosphere.

The T-peel strength of nanocomposite adhesive to the nonpolar polyolefin films (the surface was pretreated by corona discharge) was performed by the Instron tension meter Model 3367. The nanocomposite adhesive was coated on two films and allowed to dry at 60 °C for 5 min, then the two films were adhered together. The size of specimens prepared was 100 mm × 25 mm. The T-peel strength was obtained of an average of three specimens. The high temperature cooking resistance experiment was carried out at 120 °C under 0.2–0.3 MPa vapor atmosphere for 30 min.

3. Results and discussion

3.1. DSC analysis

The DSC thermograms of pure WPU and SiO_2/FWPU-15 are illustrated in Fig. 3, corresponding to curve (a) and curve (b), respectively. In the pure WPU, the glass transition temperature (T_g) of the hard segment at 39.2 °C has been observed. And the

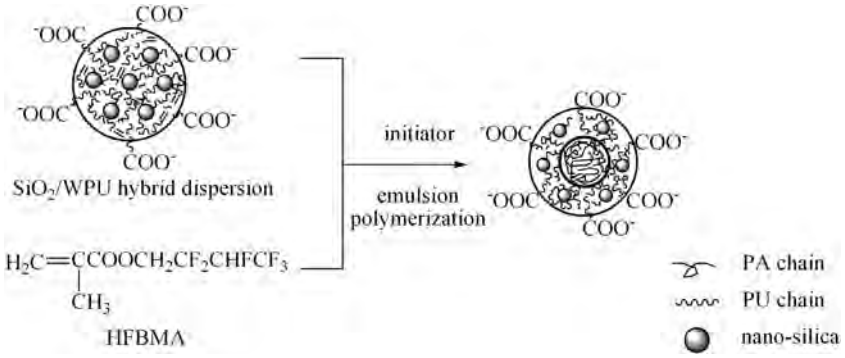

Fig. 2. Schematic illustration of the formation of SiO_2/FWPU nanocomposite particle.

Table 1
Compositions of the SiO_2/FWPU nanocomposite.

Sample	Nano-SiO_2[a] (wt%)	HFBMA[b] (wt%)	Sample	Nano-SiO_2[a] (wt%)	HFBMA[b] (wt%)
SiO_2-0/FWPU	0		SiO_2/FWPU-0		0
SiO_2-0.5/FWPU	0.5		SiO_2/FWPU-5		5
SiO_2-1/FWPU	1	15	SiO_2/FWPU-10	1	10
SiO_2-1.5/FWPU	1.5		SiO_2/FWPU-15		15
SiO_2-2/FWPU	2		SiO_2/FWPU-20		20

[a] Based on the solid content of PU prepolymer.
[b] Based on the solid content of SiO_2/WPU hybrid dispersion.

sharp melting endothermic peak around 54 °C is due to the crystalline soft segment. However, the T_g of soft segment is too low to be observed from the curve (a). Comparatively, both of the T_g of hard segment and the melting endothermic peak in SiO_2/FWPU-15 shift to a lower temperature of 34.6 and 50.3 °C, respectively, and the intensity of melting endothermic peak decreases. This is because that the C=C groups in fluorinated acrylate and PU chains react with each other during the seed emulsion polymerization process, and the compatibility between core regions and shell regions is consequently improved due to the formation of chemical linkages. As a result, the T_g of core region overlaps with the T_g of hard segment in shell region and shifts to a lower temperature, and the crystallization ability of soft segment in shell region decreases.

3.2. Emulsion properties

Fig. 4 shows the dependence of the surface tension on the concentration of SiO_2/FWPU nanocomposite emulsion. It is observed that the surface tension of diluted emulsion decreases with the increasing concentration of nanocomposite emulsion before the 0.3 wt%, and remains unchanged when the concentration is further increased. Consequently, the surface tension of diluted emulsion above the transition point (>0.3 wt%) can be regarded as the surface tension of the original SiO_2/FWPU nanocomposite emulsion. The effect of HFBMA content on the surface tension of nanocomposite emulsions was also investigated. As can be seen, the nanocomposite emulsion without HFBMA has the highest surface tension. While the surface tension of the nanocomposite emulsions decreases with the adding of HFBMA; and the surface tension is the lowest when the HFBMA content is 20%.

It is well known that the adhesive strength is largely related to the wettability of the adhesive to the adhered substrate, which can be quantified by the interfacial tension: higher interfacial tension means poorer wettability. According to the Shell–Nauman empirical formula, the interfacial tension between the nanocomposite emulsion and the nonpolar polyolefin

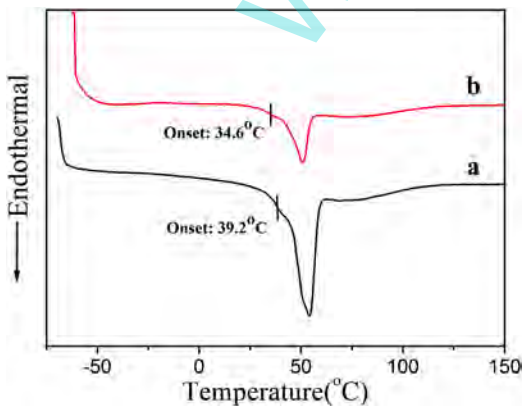

Fig. 3. The DSC thermograms of pure WPU and SiO_2/FWPU-15.

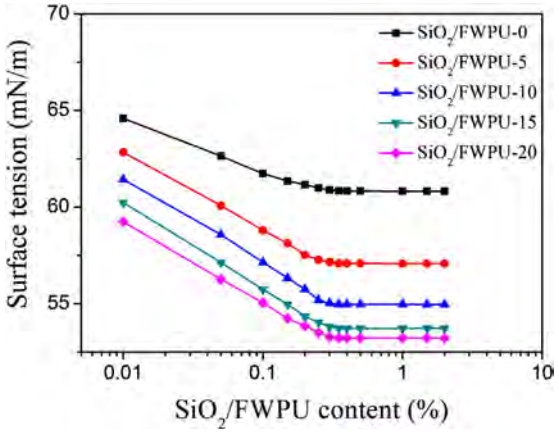

Fig. 4. Surface tension of the SiO_2/FWPU nanocomposite emulsions.

Table 2
Effect of HFBMA content on the interfacial tension between the SiO_2/FWPU nanocomposite emulsions and the nonpolar polyolefin films.

HFBMA (wt%)	PET		PE		BOPP		CPP	
	γ_{SL1}	γ_{SL2}	γ_{SL1}	γ_{SL2}	γ_{SL1}	γ_{SL2}	γ_{SL1}	γ_{SL2}
0	6.86	6.94	8.01	8.40	10.42	10.85	15.46	16.08
5	4.06	4.28	5.04	5.49	7.15	7.63	11.80	12.15
10	2.87	3.03	3.73	3.83	5.64	5.64	10.00	10.33
15	2.28	2.35	3.06	3.14	4.84	5.06	9.01	9.22
20	2.07	2.32	2.82	2.91	4.55	4.80	8.63	8.70

can be calculated as follow:

$$\gamma_{SL} = \frac{\left(\gamma_S^{0.5} - \gamma_L^{0.5}\right)^2}{1 - 0.015(\gamma_S\gamma_L)^{0.5}} \quad (2)$$

where γ_S and γ_L are the surface free energy of substrate (the measured surface tension of PET, PE, BOPP and CPP are 42.6, 40.6, 36.7 and 29.4 mN/m, respectively) and the surface tension of nanocomposite emulsion, γ_{SL} represents the interfacial tension between the nanocomposite emulsion and the substrate.

The results of γ_{SL} are listed in Table 2. It is noted that γ_{SL} decreases with the content of HFBMA, indicating that the wettability between the nanocomposite emulsion and the nonpolar polyolefin films has been improved. As mentioned previously, γ_{SL} of nonpolar polyolefin films increases in the order: PET > PE > BOPP > CPP. In fact, the calculated γ_{SL} decreases in an opposite order: CPP > BOPP > PE > PET, which is consistent with a natural expectation: the nanocomposite emulsion has better wettability to the PET film than to the CPP film, because the surface energy of the PET film is higher than that of CPP film.

The wettability can also be determined directly by the static contact angle of nanocomposite emulsion on the nonpolar polyolefin films: smaller contact angle means better wettability. As shown in Fig. 5, the measured contact angle of nanocomposite emulsion on the nonpolar polyolefin film decreases with increasing the content of HFBMA, indicating an improvement of wettability there in. And the wettability changed a little when HFBMA content was above 15%.

γ_{SL} could be calculated by the measured contact angles via the Young's equation [30,31]:

$$\gamma_S = \gamma_L\cos\theta + \gamma_{SL} \quad (3)$$

where θ is the contact angle of nanocomposite emulsion on the nonpolar polyolefin films. And the results are listed in Table 2. It is found that the γ_{SL1} calculated by the Young's equation is almost in accordance with γ_{SL2} calculated by the Shell–Nauman empirical formula. Both γ_{SL1} and γ_{SL2} show that the wettability of nanocomposite emulsion to the nonpolar polyolefin films has been improved by the HFBMA. When the HFBMA content was higher than 15%, the nanocomposite emulsion showed an excellent wetting behavior to the nonpolar polyolefin films.

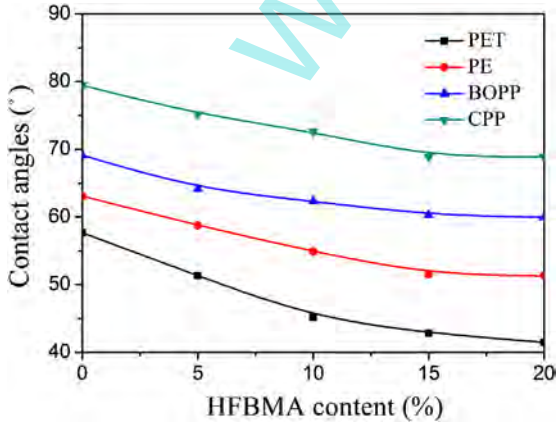

Fig. 5. The contact angles of SiO_2/FWPU nanocomposite emulsions on the laminated films.

3.3. Surface free energy and water swelling

It is important to study the surface properties of nanocomposite films. The effect of HFBMA content on the surface free energy of SiO_2/FWPU nanocomposite films was investigated by using water and ethylene glycol as standard liquids through the equation [32]:

$$(1+\cos\theta_1)\gamma_1 = 4\left(\frac{\gamma_1^d\gamma_s^d}{\gamma_1^d+\gamma_s^d} + \frac{\gamma_1^p\gamma_s^p}{\gamma_1^p+\gamma_s^p}\right) \quad (4)$$

$$(1+\cos\theta_2)\gamma_2 = 4\left(\frac{\gamma_2^d\gamma_s^d}{\gamma_2^d+\gamma_s^d} + \frac{\gamma_2^p\gamma_s^p}{\gamma_2^p+\gamma_s^p}\right) \quad (5)$$

$$\gamma_s = \gamma_s^d + \gamma_s^p \quad (6)$$

where θ_1 and θ_2 are the contact angles of water and ethylene glycol on the surface of nanocomposite film, respectively. $\gamma_s, \gamma_s^d, \gamma_s^p$ represent the surface energy, dispersion component and polar component of nanocomposite films, respectively. $\gamma_1, \gamma_1^d, \gamma_1^p$ represent the surface tension, dispersion component and polar component of water (γ_1^d = 21.8 mN/m, γ_1^p = 51.0 mN/m). $\gamma_2, \gamma_2^d, \gamma_2^p$ represent the surface tension, dispersion component and polar component of ethylene glycol (γ_2^d = 29.3 mN/m, γ_2^p = 19.0 mN/m).

The calculated results are listed in Table 3. It can be found that the contact angles of water on the nanocomposite films increased from 61.29° to 101.26°, and the surface free energy of the nanocomposite film decreased from 42.87 to 13.73 mN/m when the HFBMA content increased from 0% to 20%. And the hydrophilic nanocomposite film changed into hydrophobic film with the adding of HFBMA. The reason is that the HFBMA segments contains hydrophobic C–F groups and they are easy to migrate to the surface from the inside, which can decrease the surface free energy of nanocomposite films. However, when the HFBMA content exceeded 15%, the surface energy of the hydrophilic nanocomposite film would not decrease due to a saturation of C–F groups on the surface.

The effect of HFBMA content on the water swelling of SiO_2/FWPU nanocomposite films was also investigated, as shown in Table 3. It is evident that the water swelling of nanocomposite film decreases impressively from 19.8% to 5.1%, which proves an improvement of water resistance of nanocomposite films. First, the hydrophobicity of nanocomposite films has been improved for the C–F groups enriched on the surface. Second, the C=C groups in fluorinated acrylate can polymerize with each other to generate nanocomposite films with high cross-linking degree. Third, the – NH_2 groups on the modified nano-SiO_2 surface reacts with – NCO groups to form cross-linking polymer. These factors have improved the water resistance of the nanocomposite films.

Table 3
Surface properties of the SiO_2/FWPU nanocomposite films.

Sample	Contact angle (°)		γ_s^d (mN/m)	γ_s^p (mN/m)	γ_s (mN/m)	Swelling (%)
	H_2O	$(CH_2OH)_2$				
SiO_2/FWPU-0	61.29	54.88	4.04	38.83	42.87	19.8
SiO_2/FWPU-5	80.01	57.81	18.23	10.17	28.40	13.5
SiO_2/FWPU-10	90.88	77.54	8.53	9.67	18.20	7.5
SiO_2/FWPU-15	98.00	93.28	2.02	11.96	13.98	5.3
SiO_2/FWPU-20	101.26	86.36	9.27	4.45	13.73	5.1

3.4. XPS

The surface chemical compositions of SiO_2/FWPU nanocomposite films are also analyzed by XPS. From Fig. 6a, it can be observed that the characteristic signals of C 1s, O 1s, N 1s, Si 2p are at 284, 531, 398 and 101 eV, respectively. From Fig. 6b, there is a new characteristic signal of F 1s at 687 eV.

The XPS results are listed in Table 4. It can be found that the silicon content on the external surface of SiO_2/FWPU-0 nanocomposite films is larger than that of the bulk films. The silicon tends to migrate to external surface of the nanocomposite films for the low surface energy of Si atom. There is no fluorine group being detected in SiO_2/FWPU-0 film for the absence of HFBMA. For the SiO_2/FWPU-15 nanocomposites, it is observed that the silicon content on the external surface of the nanocomposite films is lower than that of the bulk films. While the content of fluorine on the external surface of the nanocomposite films is two times larger than that of the theoretical average fluorine content in the nanocomposite. This is because the lower surface energy of fluorine atom causes the fluorine atom to migrate to the external surface easily during the film drying process. The XPS confirmed that larger contents of fluorine migrated to external surface of the nanocomposite film, which improved the surface properties of SiO_2/FWPU nanocomposite film.

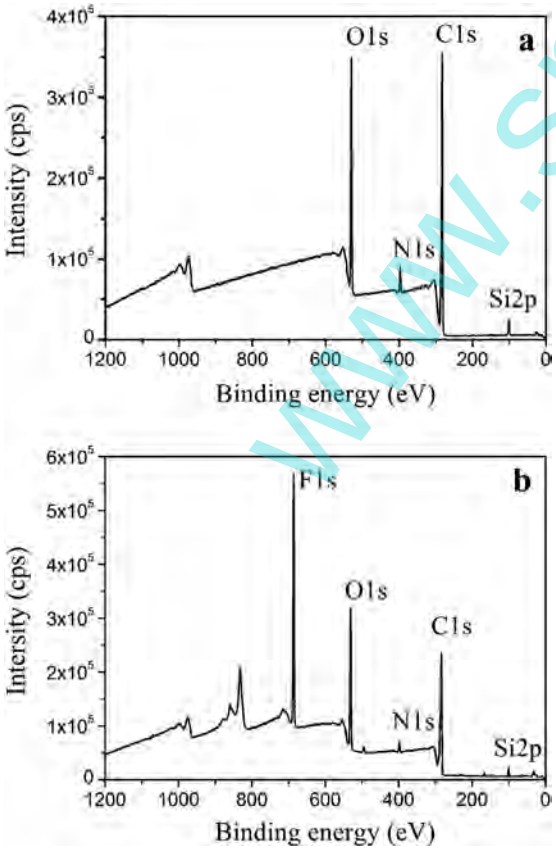

Fig. 6. XPS spectra of (a) SiO_2/FWPU-0 and (b) SiO_2/FWPU-15.

3.5. AFM

The surface morphology of pure WPU film and SiO_2/FWPU nanocomposite films was further characterized by AFM, as shown in Figs. 7 and 8. As can be seen, the surface morphology of the pure WPU film is relatively smooth, with an ordered arrangement of bright crests and dark troughs. The surface roughness of the SiO_2/FWP-0 nanocomposite film increases due to the enrichment of silicon moieties on the surface caused by modified nano-SiO_2. This might suggests that the silicon-containing segments can migrate to the film interface easily. There is no fluorine group in the SiO_2/FWPU-0 for the absence of HFBMA. The surface morphology of SiO_2/FWPU-15 nanocomposite film is very rough with a quantity of summits arranged intricately, which could be observed in the three-dimensional image (Fig. 8). It is inferred that the stiff summits distributed on the surface were corresponded to the fluorine atoms. This is because that the fluorine atoms are easy to migrate to the film interface during the film drying process, due to lower surface energy of fluorine atom in comparing to silicon atom. The AFM results are consistent with the XPS results.

3.6. TGA

The thermogravimetric analysis was carried out to investigate the effect of modified nano-SiO_2 content on the thermal stability of SiO_2/FWPU nanocomposite films. The TGA curves and differential weight loss (DTG) curves were showen in Figs. 9 and 10, respectively. The weight loss in the temperature range of 75–250 °C is attributed to the vaporization of residual water, the loss of oligomers, by-products and the silane coupling agent APTES in the nanocomposite films [33]. A better discernment of weight losses before 250 °C is shown in Fig. 9. It is observed that the weight loss of nanocomposite film increases with increasing content of modified nano-SiO_2, which is attributed to increase amount of APTES grafted on the nano-SiO_2. The weight loss in the temperature range 250–370 °C was associated with the decomposition of urethane bonds in hard segments. While the weight loss in the temperature range 370–500 °C was attributed to the scission of PBA in soft segments [34–36]. It was observed that the TGA curve

Table 4
The surface element content of SiO_2/FWPU nanocomposite films.

Element	SiO_2/FWPU-0		SiO_2/FWPU-15	
	Bulk (%)	Surface (%)	Bulk (%)	Surface (%)
C1s	72.75	67.66	56.05	44.18
O1s	22.34	26.40	25.53	19.71
N1s	3.92	3.55	1.93	1.94
F1s	–	–	15.66	33.43
Si2p	0.99	2.39	0.83	0.74

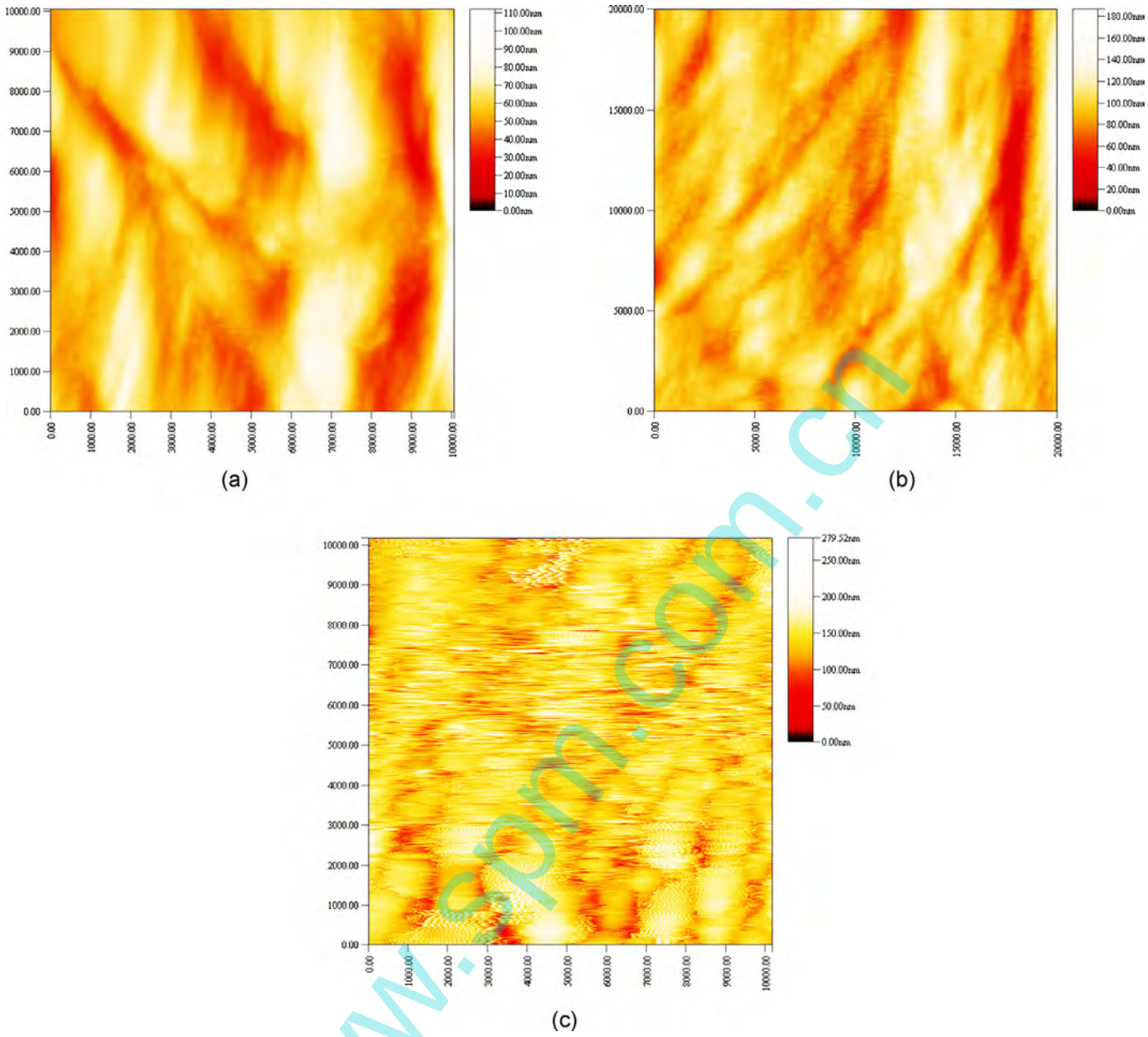

Fig. 7. Surface images of (a) WPU (b) SiO_2/FWPU-0 (c) SiO_2/FWPU-15.

of nanocomposite films shifted toward to higher temperature range with increasing the modified nano-SiO_2 content. And the char residue after 550 °C increases with content of inorganic SiO_2.Furthermore, the DTG curves reveals a two-stage degradation of hard segments and soft segments, which were not clear in the TGA curves. It found that degradation peaks shifted to a higher temperature. Both the TGA and the DTG results indicated that the thermal stability of nanocomposite films was enhanced. It is ascribed to several factors. First, the nano-SiO_2 particles act as thermal insulator and mass transport barrier, which prevents the heat transfer and the permeability of volatile products from generating in the degradation process. Second, the increased cross-linking density of the products by adding functional nano-SiO_2 will improve the thermal stability of nanocomposite films. Third, the bond energy of Si–O is higher than that of C–O, resulting in an improvement of thermal stability of nanocomposite films. In a word, the modified nano-SiO_2 can enhance the thermal stability of SiO_2/FWPU nanocomposite films.

3.7. Adhesive property

The adhesives for the laminated soft package films should have excellent adhesive strength, outstanding water resistance and thermal stability. The effect of HFBMA content on the adhesion strength of adhesive to the nonpolar polyolefin films was studied, as shown in Fig. 11. It can be seen that the adhesion strength increased with increasing content of HFBMA. This is because that the adhesive strength depends on the wettability between the adhesive and adhered substrate. An excellent wettability could ensure the close contact between the adhesive and adhered substrate, and this increases the absorption of adhesive to the substrate. In order to get good adhesive strength, there should be no gas between the adhesive and the substrate. The adhesive strength was improved with the adding of HFBMA. However, the adhesion strength tended to be constant when the HFBMA content is higher than 15%, because the wettability was only influenced by the HFBMA content. The best adhesion strength was found in PET/

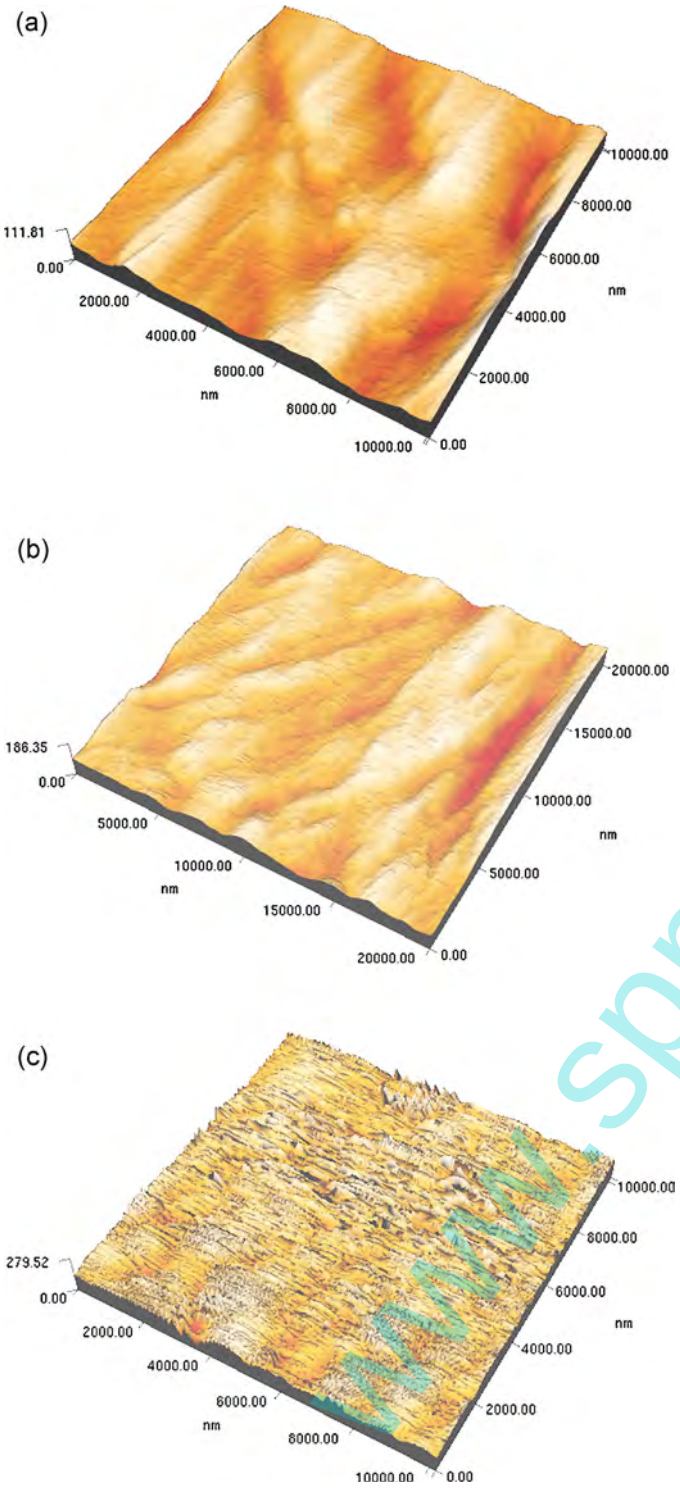

Fig. 8. Three-dimensional images of (a) WPU (b) SiO_2/FWPU-0 (c) SiO_2/FWPU-15.

PET, because the wettability was the highest between the nanocomposite emulsion and the PET film, as explained earlier.

The effect of content of modified nano-SiO_2 on the adhesion strength of nanocomposite adhesives to the nonpolar polyolefin films at room temperature and under high temperature cooking atmosphere was studied, as shown in Fig. 12a and b, respectively.

In Fig. 12a, there was no obvious influence of the modified nano-SiO_2 content on the T-peel strength, and SiO_2-1/FWPU nanocomposite adhesive exhibited a good adhesive strength. However, the adhesion strengths decreased after steaming at

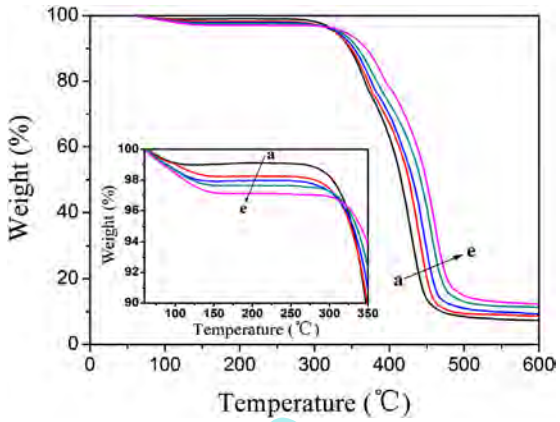

Fig. 9. TGA curves of the SiO_2/FWPU composites with different SiO_2 content (a) 0% (b) 0.5% (c) 1% (d) 1.5% (e) 2%.

120 °C for 30 min, as shown in Fig. 12b. This might be the poor water resistance of nanocomposite adhesive caused by the hydrolysis of polyester PBA in the soft segments, which decreases the cohesive strength of nanocomposite adhesive. However, the adhesion strength decreases a little with the increasing nano-SiO_2 content. The water resistance and thermal stability of nanocomposite films have been improved. On one hand, the cross-linking density in the nanocomposite films increases with the adding of nano-SiO_2, which prevents water vapor from permeating into the films. And the nano-SiO_2, acting as a thermal insulator, could decrease the heat transfer. Another reason is the adding of the HFMBA. As mentioned earlier, the water resistance of nanocomposite film was improved by adding the HFBMA. During the high temperature steaming process, the water vapor was difficult to penetrate into the film to hydrolyze the ester groups. As a result, the adhesive strength decreased a little for the improved water resistance and thermal stability. However, the adhesive strength of nanocomposite adhesive decreased when nano-SiO_2 content was above 1%. This might due to the aggregation of the nano-SiO_2 above the critical content, which increases the voidage of nanocomposite film. Which allows permeation of water vapor and accordingly hydrolysis of ester groups, resulting in the decrease of adhesive strength of nanocomposite adhesive.

3.8. Empirical model

Taking into consideration all aspects of the previous discussion, we develop an empirical model that correlates the adhesion

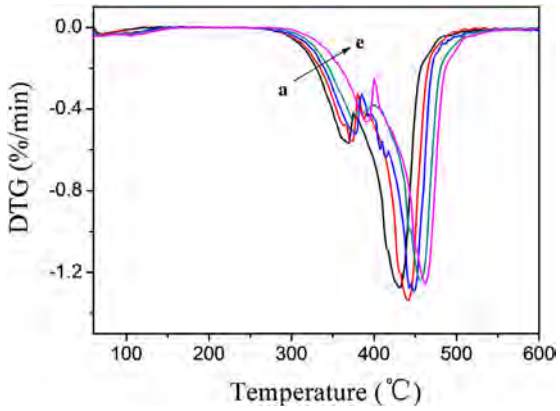

Fig. 10. DTG curves of the SiO_2/FWPU nanocomposites with different SiO_2 content (a) 0% (b) 0.5% (c) 1% (d) 1.5% (e) 2%.

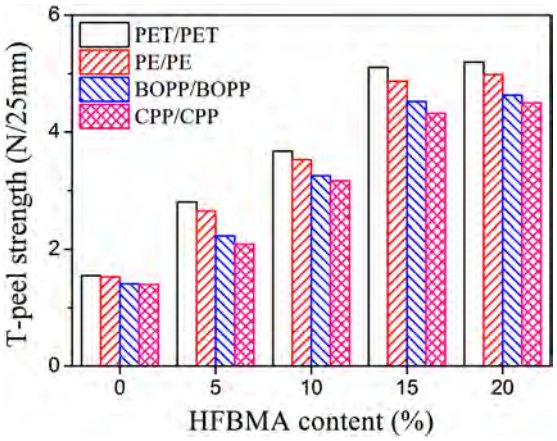

Fig. 11. Effect of HFBMA content on the T-peel strength of laminated films at 25 °C.

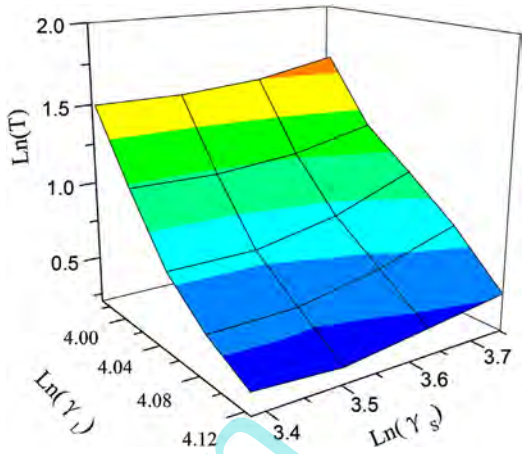

Fig. 13. The three-dimensional schematic of empirical model.

strength, the surface tension of nanocomposite adhesive and the surface free energy of adhered substrate. Since the surface tension of nanocomposite adhesive is greatly affected by the HFBMA content, the adhesion strength results obtained from the effect of HFBMA content on the T-peel strength of nonpolar polyolefin films at 25 °C are used to build the empirical model. The three-dimensional schematic of the empirical model is shown in Fig. 13.Under this circumstance, the empirical equation is defined as the form:

$$T = \lambda \times \gamma_L^{\alpha} \times \gamma_S^{\beta} \tag{7}$$

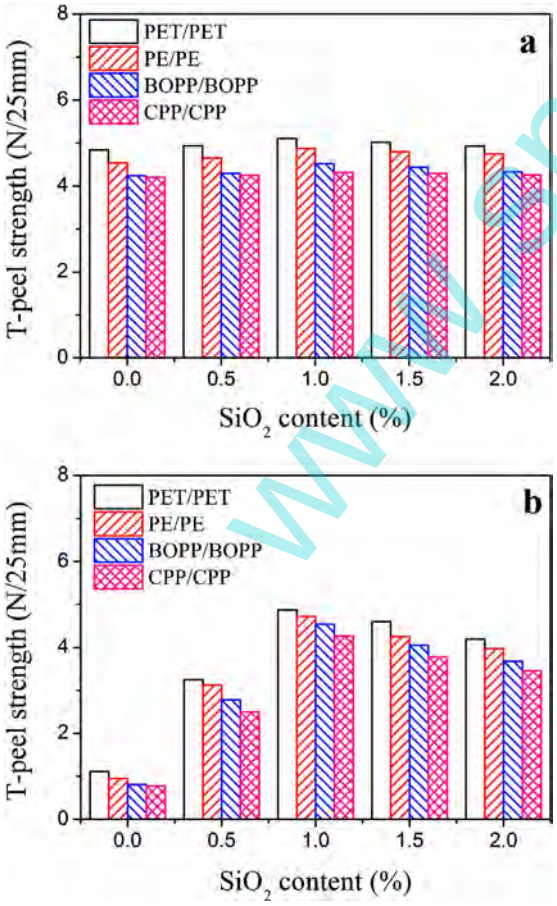

Fig. 12. Effect of nano-SiO_2 content on the T-peel strength of laminated films (a) at 25 °C (b) cooking at 120 °C and 0.2–0.3 MPa vapor atmosphere for 30 min.

where λ, α, β are the constant coefficient, exponential coefficients of γ_L and γ_S, respectively. T is the T-peel strength. Then Eq. (7) is taken the log on both side and given by:

$$\mathrm{Ln}(T) = \mathrm{Ln}(\lambda) + \alpha\,\mathrm{Ln}(\gamma_L) + \beta\,\mathrm{Ln}(\gamma_S) \tag{8}$$

The SPSS 11.01 software was employed to fit Eq. (8) by multiple linear regressions. The fitted results of coefficients were λ =e xp (32.04), $\alpha = -8.08$ and $\beta = 0.45$, then we have Eq. (9):

$$T = e^{32.04} \times \gamma_L^{-8.08} \times \gamma_S^{0.45} \tag{9}$$

For this empirical model, it was surprisingly observed that the correlation coefficient R between the actual T and the predicted one was quite close to 1, i.e. $R = 0.996$, which confirms the validity of the present model. According to the Fig. 12 and Eq. (9), it can be inferred that an effective way to improve the adhesion strength would be either to decrease γ_L or to increase γ_S.

4. Conclusion

A series of high performance adhesives used for the laminated soft package films were made by the SiO_2/FWPU nanocomposite emulsions, and the influences of contents of modified nano-SiO_2 and HFBMA on the improved adhesion were analyzed. The experimental results showed that the wetting behavior, water resistance and thermal stability of nanocomposite adhesive were suggested as key factors for the improved adhesion strength. It was also concluded that the nanocomposite adhesive could be applied on the nonpolar polyolefin films and meets the requirement of high adhesive strength under high temperature cooking atmosphere in the laminated soft package field. In addition, the nanocomposite adhesive exhibited an optimized adhesive strength when the modified nano-SiO_2 content was 1% and the HFBMA content was 15%.

An empirical model developed to correlate the adhesion strength to the surface tension of adhesive and the surface energy of adhered substrate was developed. The model provide a simple way in predicting the adhesion strength, which would contribute to our understanding of the adhesion mechanism.

Acknowledgments

We appreciate the financial support from the National Natural Science Foundation of China under grant No. 21171058.

References

[1] M. Aznar, P. Vera, E. Canellas, C. Nerín, P. Mercea, A. Störmer, Journal of Materials Chemistry 21 (2011) 4358.

[2] P. Mareri, S. Bastide, N. Binda, A. Crespy, Composites Science and Technology 58 (1998) 747–752.
[3] N. Kalapat, T. Amornsakchai, Surface and Coatings Technology 207 (2012) 594–601.
[4] S. Haridoss, M.M. Perlman, Journal of Applied Physics 55 (1984) 1332–13381338.
[5] A. Viraneva, T. Yovcheva, M. Hristov, G. Mekishev, IEEE Transactions on Dielectrics and Electrical Insulation 19 (2012) 1132–1136.
[6] A.N. Hammoud, J.R. Laghari, B. Krishnakumar, IEEE Transactions on Nuclear Science 35 (1988) 1026–1029.
[7] S.P. Cygan, J.R. Laghari, IEEE Transactions on Nuclear Science 38 (1991) 906–912912.
[8] A.M. Abdul-Kader, Y.A. El-Gendy, A.A. Al-Rashdy, Radiation Physics and Chemistry 81 (2012) 798–802.
[9] D.K. Lee, H.B. Tsai, H.H. Wang, R.S. Tsai, Journal of Applied Polymer Science 94 (2004) 1723–1729.
[10] J.L. Zhang, D.M. Wu, D.Y. Yang, F.X. Qiu, Journal of Polymers and the Environment 18 (2010) 128–134.
[11] L. Wang, Y. Shen, X. Lai, Z. Li, Journal of Applied Polymer Science 119 (2011) 3521–3530.
[12] K.K. Jena, S. Sahoo, R. Narayan, T.M. Aminabhavi, K. Raju, Polymer International 60 (2011) 1504–1513.
[13] M. Rostami, M. Mohseni, Z. Ranjbar, International Journal of Adhesion and Adhesives 34 (2012) 24–31.
[14] Z.S. Petrović, Y.J. Cho, I. Javni, S. Magonov, N. Yerina, D.W. Schaefer, J. Ilavský, A. Waddon, Polymer 45 (2004) 4285–4295.
[15] M. Rostami, M. Mohseni, Z. Ranjbar, Pigment & Resin Technology 40 (2011) 363–373.
[16] X. Li, Z. Cao, Z. Zhang, H. Dang, Applied Surface Science 252 (2006) 7856–7861.
[17] Z. Li, Y. Zhu, Applied Surface Science 211 (2003) 315–320.
[18] C. Takai, M. Fuji, M. Takahashi, Colloids and Surfaces A: Physicochemical and Engineering Aspects 292 (2007) 79–82.
[19] H.D. Hwang, H.J. Kim, Journal of Colloid and Interface Science 362 (2011) 274–284.
[20] V. Castelvetro, F. Ciardelli, G. Francini, P. Baglioni, Macromolecular Materials and Engineering 278 (2000) 6–16.
[21] F. Levine, J. La Scala, W. Kosik, Progress in Organic Coatings 69 (2010) 63–72.
[22] H.W. Bonk, A.A. Saidanpoli, H.J. Ulrich, Elastoplast 3 (1971) 157.
[23] H.F. Mark, P.J. Debye, in: P. Weiss (Ed.), Adhesion and Cohesion, Elsevier, New York, 1962, p. 240.
[24] H. Grimeley, Aspects Adhesion 7 (1973) 11.
[25] D.D. Eley, Adhesion, London Oxford University Press, Oxford, UK, 1961.
[26] J. Tyczkowski, I. Krawczyk-Kłys, S. Kuberski, P. Makowski, European Polymer Journal 46 (2010) 767–773.
[27] M. Li, Z. Zheng, S. Liu, Y. Su, W. Wei, X. Wang, International Journal of Adhesion and Adhesives 31 (2011) 565–570.
[28] D. Mishra, V. Kumar Sinha, International Journal of Adhesion and Adhesives 30 (2010) 47–54.
[29] F. Gao, B. Ku, S. Huang, Journal of Applied Polymer Science 122 (2011) 798–803.
[30] M.J. Geerken, R.G.H. Lammertink, M. Wessling, Colloids and Surfaces A: Physicochemical and Engineering Aspects 292 (2007) 224–235.
[31] P.R. Waghmare, S.K. Mitra, Langmuir 26 (2010) 17082–17089.
[32] L. Jiang, Y.L. Chen, C.P. Hu, Journal of Coatings Technology and Research 4 (2007) 59–66.
[33] J.M. Yeh, C.T. Yao, C.F. Hsieh, H.C. Yang, C.P. Wu, European Polymer Journal 44 (2008) 2777–2783.
[34] A. Patel, C. Patel, M.G. Patel, M. Patel, A. Dighe, Progress in Organic Coatings 67 (2010) 255–263.
[35] J.M. Cervantes-Uc, J.I.M. Espinosa, J.V. Cauich-Rodríguez, A. Ávila-Ortega, H. Vázquez-Torres, A. Marcos-Fernández, J. San Román, Polymer Degradation and Stability 94 (2009) 1666–1677.
[36] Y. Zhang, P. Zhang, X. Chen, Z. Wu, Q. Wu, Industrial & Engineering Chemistry Research 50 (2011) 2111–2116.